scientific reports

Check for updates

OPEN

IGF-1 regulates cancer cell immune evasion in prostate cancer

Ashwin M. Nandakumar[1]✉, Alessandro Barberis[1,8], Jinseon Kim[1,8], Cameron R. Lang[2], Jack V. Mills[1], Guillaume Rieunier[2], Dimitrios Doultsinos[1], Avigail Taylor[1], Ashwin Jainarayanan[3], Su M. Phyu[2], Leticia Campo[2], Alistair Easton[2], Eileen E. Parkes[2], Timothy James[4], Freddie C. Hamdy[1], Clare Verrill[1,5], Ian G. Mills[1] & Valentine M. Macaulay[1,6,7]

Insulin-like growth factor-1 (IGF-1) is associated with prostate cancer (PCa) development and lethality and exhibits immunosuppressive properties in other models. We investigated IGF-1's tumor-intrinsic immune effects in PCa to understand mechanisms underlying its poor immunotherapy response. Transcriptional profiling of human (DU145, 22Rv1) and murine (Myc-CaP) PCa cells revealed that IGF-1 suppresses cytokine signalling, antigen processing and presentation, and additional immune regulatory pathways. We further examined the expression of components involved in cancer cell recognition and immune evasion: the antigen processing machinery and PD-L1 checkpoint. IGF-1 downregulated key elements such as transporters associated with antigen processing (TAPs), endoplasmic reticulum aminopeptidase-1 (ERAP-1), and Class I β2-microglobulin, without significantly altering Class I allele expression. These changes were associated with reduced surface presentation of Class I complexes on Myc-CaP cells, suggesting disrupted peptide transport, processing, and/or presentation. In contrast, IGF-1 upregulated the immune checkpoint CD274 (PD-L1) via IGF receptor/AKT/ERK-dependent signalling. Analysis of TCGA Firehose Legacy PCa data showed higher CD274 expression in tumors with elevated IGF1 and IGFBP5. Multiplex immunofluorescence in primary PCa confirmed increased PD-L1 in patients with high serum IGF-1, supporting its role in immune evasion. Overall, these findings reveal a novel IGF-1-driven immunosuppressive mechanism that may underlie PCa's resistance to immunotherapy.

Insulin-like growth factors (IGFs) promote normal development and contribute to the growth and spread of cancers, primarily mediated by activation of type 1 IGF receptors (IGF-1Rs)[1]. We previously showed that IGF-1Rs are overexpressed in primary prostate cancer (PCa) and are further upregulated on progression to androgen-independent metastatic disease[2,3]. IGF-1 also influences cancer risk: men with high serum IGF-1 have increased risk of PCa development and lethality, with evidence of a causative association[4,5]. Although many pro-tumorigenic effects of IGF axis activation are mediated via IGF-1Rs expressed by target epithelial, mesenchymal, and endothelial cells, it is increasingly recognized that IGFs also influence anti-tumor immunity. IGF-1 promotes the function of immunosuppressive FOXP3 + regulatory T-cells (Tregs) and enhances T-cell secretion of cytokines including IL10, required for macrophage polarization to the pro-tumorigenic, immunosuppressive M2 phenotype[6–8]. These factors may contribute to the strongly immunosuppressive tumor microenvironment (TME) of PCa and poor response to immune checkpoint blockade (ICB)[9].

Cancers can evade detection by the adaptive immune system by suppressing cell surface presentation of antigenic peptides. Generally, aberrant cells are recognized by the presence of short peptides generated in the proteasome, transported into the endoplasmic reticulum (ER) by transporters associated with antigen processing (TAP1/2), trimmed by ER aminopeptidases (ERAPs) to modify affinity for Class I molecules, and loaded onto Class I heterodimers comprising a polymorphic heavy α-chain and an invariant β2-microglobulin (β2M) light chain for presentation at the cell surface[10,11]. Many cancers including PCa downregulate cell surface Class I[12]; it was shown 30 years ago by Trojan and colleagues that this defect could be rescued in rat high grade glioma (HGG) cells by IGF-1 depletion, rendering the cells non-tumorigenic and able to induce CD8 + cytotoxic T-cell

[1]Nuffield Department of Surgical Sciences, University of Oxford, Oxford, UK. [2]Department of Oncology, University of Oxford, Oxford, UK. [3]Nuffield Department of Orthopedics, Rheumatology and Musculoskeletal Sciences, Kennedy Institute of Rheumatology, The University of Oxford, Oxford, UK. [4]Department of Biochemistry, Oxford University Hospitals NHS Foundation Trust, Oxford, UK. [5]Department of Cellular Pathology, Oxford University Hospitals NHS Foundation Trust, Oxford, UK. [6]Oxford Cancer Centre, Churchill Hospital, Oxford, UK. [7]Valentine M. Macaulay is deceased. [8]Alessandro Barberis and Jinseon Kim: These authors contributed equally to this work. ✉email: ashwin.nandakumar@nds.ox.ac.uk

infiltration and regression of unmodified tumors in syngeneic animals[13]. Similar immune-mediated tumor regression was reported in rats injected with IGF-1R-depeted HGG cells, findings that triggered a pilot clinical trial and a Phase IIb trial (NCT04485949)[14–16].

Clinical evidence for IGF-associated immunosuppression comes from reports of low tumor infiltrating lymphocytes (TILs) in high IGF-1R PCa bone metastases, and genomic aberrations in cancer patients with hyper-progressive disease post-ICB, including mutations in negative IGF regulator *IGFBP2* and transcriptional upregulation of IGF-1, PI3K-AKT and ERK pathways[17,18]. More recently, short-term starvation was shown to sensitize non-small cell lung cancer (NSCLC) to PD-1 blockade in vivo by suppressing serum IGF-1 and IGF-1R activity in tumor tissue. Furthermore, NSCLC patients with durable clinical benefit post-ICB had significantly lower circulating IGF-1 and lower tumor IGF-1R than those with no durable benefit[19]. IGF-1R inhibition is also reported to enhance responses to anti-PD-1 in colorectal cancer and triple negative breast cancer[20,21]. These findings prompted us to investigate the hypothesis that IGF-1 has immunosuppressive actions in prostate cancer epithelium contributing to cancer cell immune evasion.

Results

IGF-enriched pathways include activated cell cycle, DNA replication and repair and suppressed immune pathways

As a first step to investigate associations of IGF axis components with immune factors, we analyzed effects of IGF-1 on gene expression in three PCa cell lines: two human, androgen receptor (AR)-positive 22Rv1 cultured from a xenograft established from primary PCa, and AR-negative DU145 derived from metastatic cancer; and one murine, Myc-CaP, derived from primary adenocarcinoma in the Hi-Myc mouse[22]. Sub-confluent cultures were serum-starved for 24 h and treated with IGF-1 or solvent (control) for 24 h prior to RNA extraction. We identified 3,471 differentially regulated genes (DEGs) in DU145, 2,321 in 22Rv1 and 600 Ensembl notations corresponding to 584 gene IDs in Myc-CaP (Supplementary Tables S4-6, Supplementary Figure S1). Variation in the numbers and identity of IGF-regulated genes may reflect differences in AR status and potentially the dominance of Myc transcriptional programming in Myc-CaP cells[23]. There were 31 significantly upregulated DEGs and 26 downregulated DEGs in common between the 3 cell lines (Fig. 1A). These included 5 genes in the COSMIC Cancer Gene Census of mutated genes implicated as cancer drivers (Supplementary Table S7), and 12 upregulated and 10 downregulated genes associated with immune-relevant pathways (Fig. 1B).

Initial unbiased enrichment analysis highlighted activation of cell cycle, DNA replication and repair, and metabolism -related pathways (Supplementary Tables S8-10). IGF-induced regulation of these pathways is well documented[1], providing confidence that the cells generated expected responses to IGF-1. Enrichment analysis also identified pathways less well-recognized as IGF-related, including immune regulator-associated pathways, almost all with negative enrichment scores suggesting pathway inactivation (Supplementary Tables S8-10). This finding prompted us to perform focused enrichment analysis on pathways related to three broad categories of immune function (Supplementary Table 11). These were production of and response to cytokines and chemokines, antigen processing machinery (APM), and other immune response-related pathways including checkpoint regulation.

The enrichment pattern varied between cell lines, with predominant association with immune response-related in DU145, cytokine signaling in 22Rv1, and immune response-related in Myc-CaP cells (Fig. 1C, Supplementary Table S12). Myc-CaP cells also has the highest number of antigen processing and presentation-related enrichment hits among the three cell lines. Figure 1D shows a heatmap of enriched pathways and enrichment scores for each cell line. Amongst cytokine-related pathways, the cellular response to interferon gamma (IFNγ) was suppressed in all 3 cell lines (Fig. 1E). General 'immune-related' pathways included regulation of JNK cascade, inactivated in all 3 cell lines, and 'systemic lupus erythematosus', activated in DU145 and 22Rv1 and containing many complement, Fc receptor and HLA encoding genes (www.genome.jp/entry/pathway+hsa05322). There was also enrichment of APM-related pathways, apparently activated in the human cells but suppressed in Myc-CaP (Fig. 1D-E).

IGF-1 influences expression of genes that regulate protein degradation, peptide processing and presentation

Defects in antigen presentation have been described in PCa cell cultures[24], involving multiple components of the APM. Defective APM results in cancer cell immune evasion, diminishing the effectiveness of immunotherapy. Having identified IGF-enriched immune pathways related to antigen processing and presentation (Fig. 1D-E) we assessed effects of IGF-1 on expression of genes that regulate intracellular protein degradation, peptide processing and presentation. First we assessed proteolytically active proteasome subunits *MECL1*, *LMP2* and LMP7 required for assembly of the 20 S proteasome, protein degradation and amino acid recycling[25], finding IGF-induced *MECL1* downregulation in DU145 cells only and *LMP2* downregulation in both DU145 and 22RV1 (Supplementary Figure S2A). In all three cell lines lysosome-associated membrane protein 2 (*LAMP2*), which maintains lysosomal integrity and function, was downregulated by IGF-1; indeed low *LAMP2* reportedly associates with adverse overall survival in high-grade PCa[26]. RB1-inducible coiled-coil protein 1 *(RB1CC1)*, an ULK1 complex component required for autophagy induction, was also coordinately downregulated. Autophagy-related genes *ATG14 and VTI1B* are required for autophagosome formation; *ATG14* was downregulated in 22Rv1 and Myc-CaP, and *VTI1B* in 22Rv1 only (Supplementary Figure S2B-C). These data suggest that IGF-1 may influence protein/peptide degradation via lysosomal and/or autophagic pathways.

We then assessed genes encoding regulators of peptide transport, processing and presentation. In all three cell lines IGF-1 caused significant *TAP1*, *TAP2* and *ERAP1* downregulation, accompanied in Myc-CaP by downregulation of TAP binding protein *Tapbp* (Fig. 2A-B, Supplementary Figure S3A). Although we identified IGF-induced deregulation of pathways related to antigen presentation (Fig. 1D), IGF-1 had little effect on

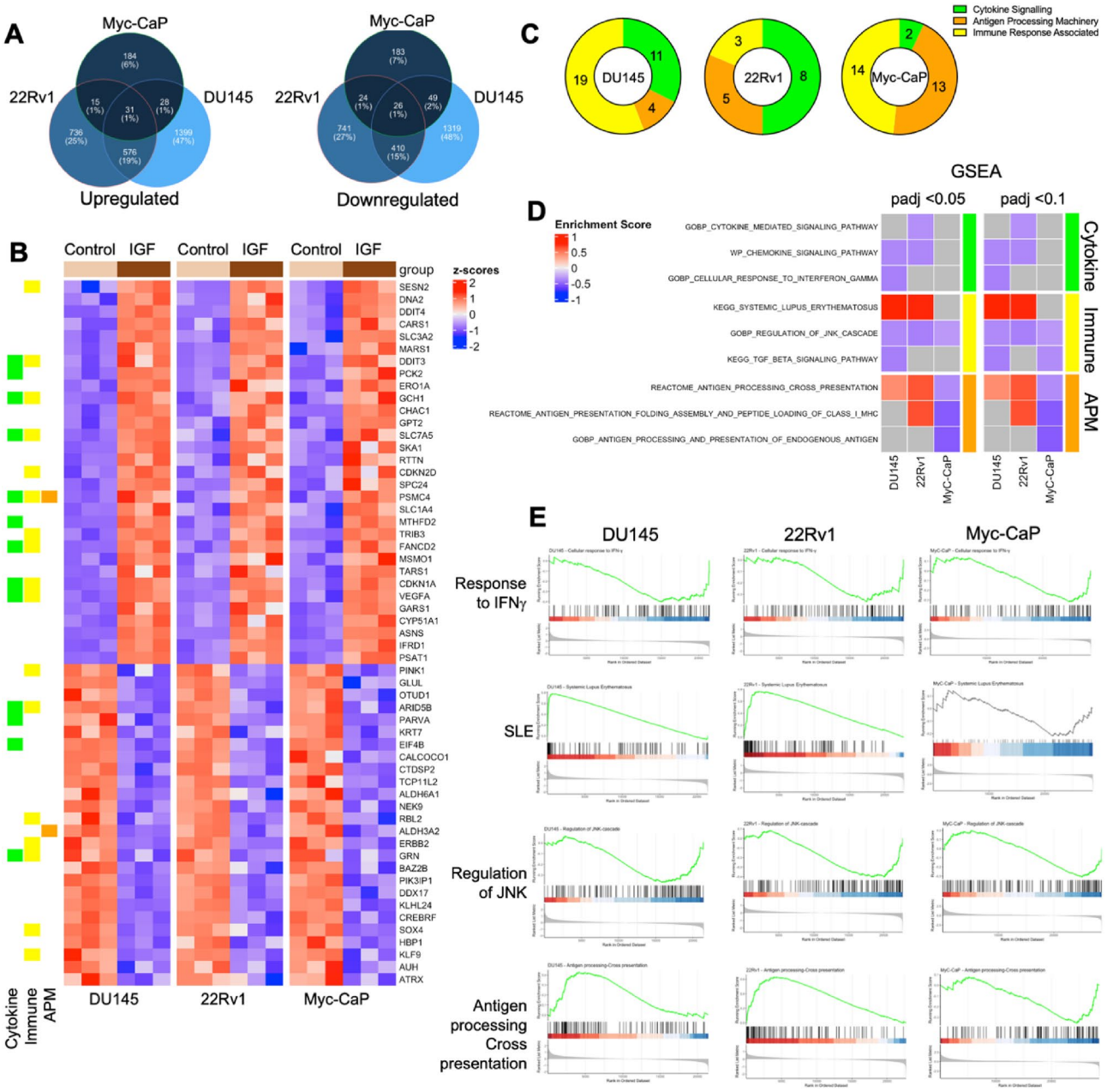

Fig. 1. IGF-1 deregulates immune-associated genes and transcriptional pathways. Subconfluent DU145, 22Rv1 and Myc-CaP cultures were serum-starved for 24 h, stimulated with 30 nM IGF-1 or solvent (control) for 24 h and RNA was extracted for RNA-seq. **A.** IGF-induced DEGs unique to and shared between the 3 PCa cell lines showing number (%). **B.** Expression heatmap of 57 DEGs in common between the 3 cell lines including 31 significantly upregulated and 26 downregulated DEGs and annotation into three curated immune relevant categories: cytokine signaling, immune response associated and Antigen Processing Machinery (APM). **C.** GSEA was performed using the three curated immune-associated pathway datasets (Supplementary Table S11). Pie charts represent the distribution of enriched pathways in each cell line. **D.** Heatmap of selected enriched pathways and enrichment scores at padj < 0.05 and < 0.01 for each cell line. **E.** GSEA enrichment plots showing response to interferon gamma (IFNγ), systemic lupus erythematosus (SLE), regulation of JNK cascade and antigen processing and cross presentation.

expression of genes encoding MHC Class I α-chains themselves, the only significant effect being apparent *HLA-C* upregulation in 22Rv1 (Supplementary Figure S3B-D). In contrast, β2m was significantly downregulated by IGF-1 in all 3 cell lines (Fig. 2C). Given identification of enriched APM pathways in IGF-treated Myc-CaP cells (Fig. 1B), we used Myc-CaP to assess potential consequences for antigen presentation. Cell surface Class I complexes (H-2Kq) were detectable in ~50% of cells, with marked reduction in both % positivity and median fluorescence intensity (MFI) after 5 days exposure to IGF-1 (Fig. 2D-E, Supplementary Figure S3E-F). As the

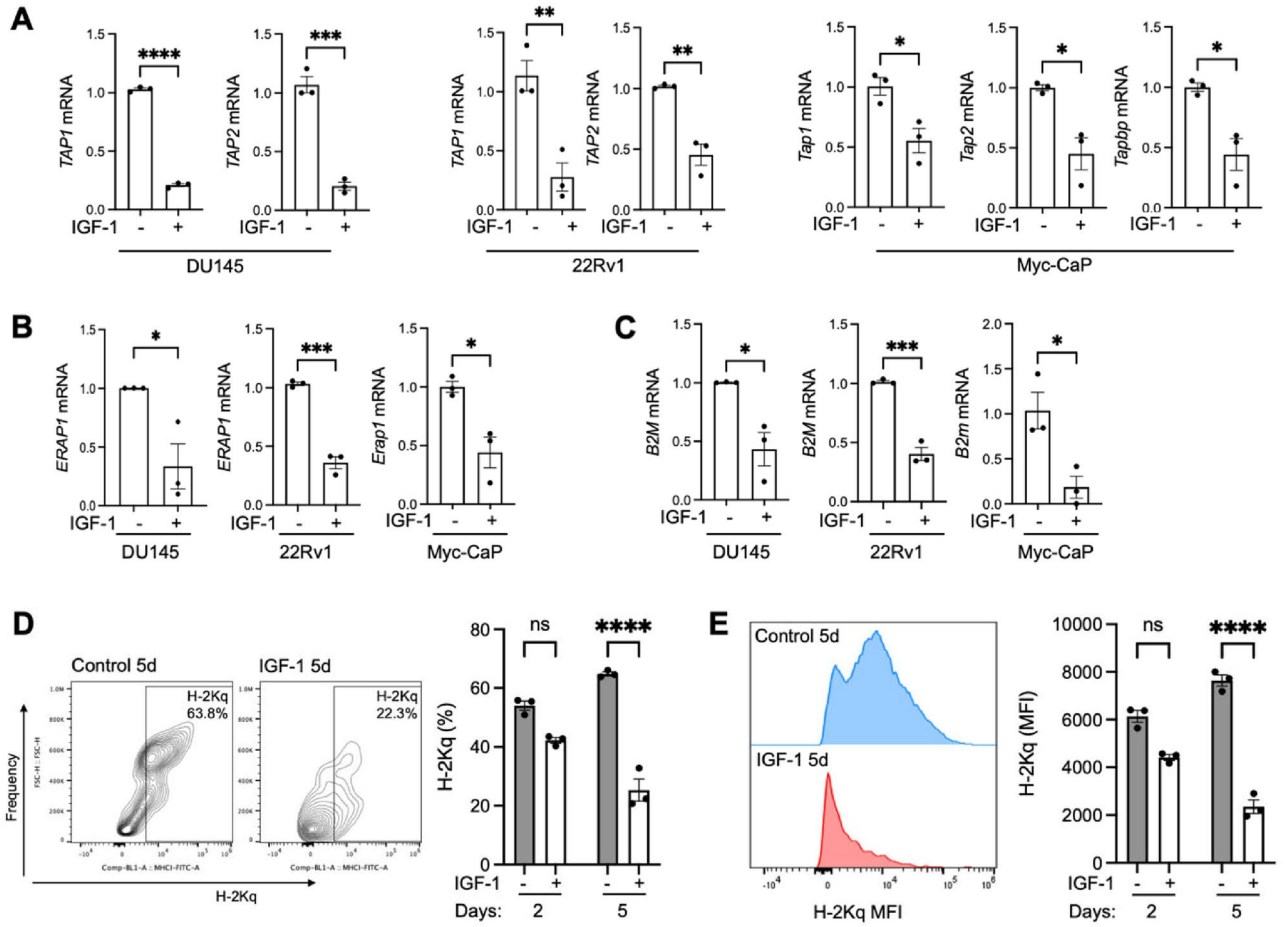

Fig. 2. IGF-1 downregulates antigen processing and presentation components. RNA was extracted from DU145, 22Rv1, and Myc-CaP cells 24 h after serum-starving and IGF-treatment as in Fig. 1, and gene expression was assessed by RT-qPCR. Expression of: **A**. *TAP1*, *TAP2* mRNA in all cell lines and *Tapbp* in MycCaP; **(B)** ERAP mRNA, **(C)**β2M mRNA. **D**, **E**. Class I complexes are stabilized at the cell surface by high affinity peptide binding, while peptide-free (empty) heterodimers are generally unstable at the cell surface at physiological temperature. We used Class I antibody to H-2Kq, appropriate to the genotype of FVB mice from which Myc-CaP cells were derived[22]. Analysis by flow cytometry of H2Kq surface expression in Myc-CaP cells treated with 30 nM IGF-1 or solvent for 2 or 5 days, showing representative flow cytometry plots at 5 days and $n = 3$ independent experiments. D: percentage H2Kq positivity, E: H2Kq MFI. All graphs represent mean ± SEM of three independent analyses (*$p < 0.05$; **$p < 0.01$; ***$p < 0.001$; ****$p < 0.0001$; ns, nonsignificant by one-way ANOVA).

H-2Kq antibody recognises properly assembled, peptide-loaded MHC class I complexes, this reduction likely reflects a functional impairment of Class I antigen presentation capacity. This effect appears to correlate with downregulation of genes encoding antigen processing components and β2M rather than downregulation of Class I genes themselves.

IGF-axis activation induces PD-L1 upregulation

In addition to a functional APM, the regulation of tumor-intrinsic immune suppressors and immune checkpoint expression are crucial for immune-mediated clearance of cancer cells. *ASS1* and *ARG1* encode enzymes that respectively regenerate and degrade arginine, which has immunosuppressive effects in the PCa microenvironment[27]. *ASS1* was downregulated in all three cell lines, *ARG1* in only DU145 (Supplementary Fig. 4A-C). There was a non-significant trend to upregulation of *VSIR*, encoding inhibitory checkpoint V-domain Ig suppressor of T cell activation (VISTA), in IGF-treated DU145 and 22Rv1 cells and no detectable *Vsir* in Myc-CaP (Supplementary Figure S4A-B). Other immune checkpoints including *CD274* (PD-L1), *PDCD1LG2* (PD-L2) and *CTLA4* were not identified as IGF-induced DEGs in any cell line, and gene counts for *PDCD1LG2* and *CTLA4* were essentially zero. However, we assessed expression of *CD274* in view of the reported ability of IGF-1R inhibition to synergize with anti-PD-1 immunotherapy[19]. In contrast to IGF-induced downregulation of multiple immune-relevant genes detected thus far (Fig. 2A-C), IGF-1 caused statistically significant upregulation of *CD274* mRNA in all three PCa cell lines (Fig. 3A). By flow cytometry, IGF-1 upregulated PD-L1 surface

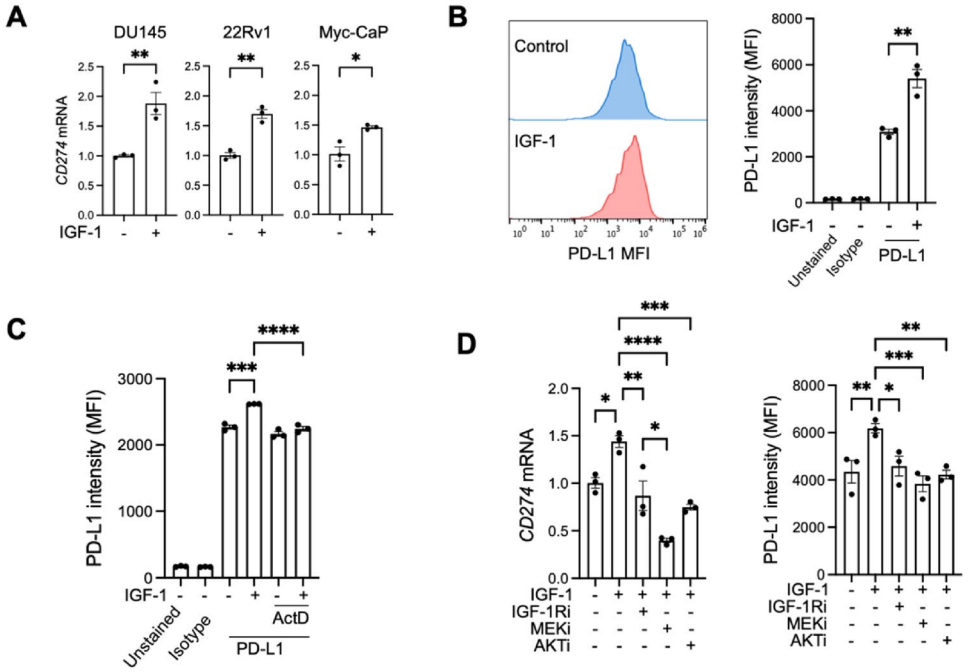

Fig. 3. IGF-1 upregulates immune checkpoint PD-L1. (A) PCa cells were serum starved for 24 h, treated with 30 nM IGF-1 or solvent and expression of *CD274* assessed by qPCR ($n = 3$ independent assays, mean ± SEM). **(B)** DU145 cells were treated as in A and PD-L1 surface expression measured by flow cytometry. Left, representative flow histogram; right, quantification of MFI ($n = 3$ independent assays, mean ± SEM). **(C)** DU145 cells were pre-treated with 1 µg/mL Actinomycin D for 2 h and then 30 nM IGF-1 was added. After 24 h PD-L1 surface expression was measured using flow cytometry. Graphs represent mean ± SEM. **(D)** DU145 cells were pre-treated with 300 nM IGF-1R inhibitor BMS-754,807, 5 µM AKT inhibitor AZD5363 and 50 nM MEK inhibitor trametinib for 1 h and 30 nM IGF-1 was added for 24 h. Parallel cultures were used for RNA extraction and RT-qPCR for *CD274* (PD-L1) mRNA quantification (upper graph) and surface protein expression measured by flow cytometry (lower, $n = 3$ independent assays, mean ± SEM). (*$p < 0.05$; **$p < 0.01$; ***$p < 0.001$; ****$p < 0.0001$; ns, nonsignificant by one-way ANOVA).

expression in DU145 cells in both serum-free and serum-supplemented media (Fig. 3B, Supplementary Figure S5A). Baseline PD-L1 surface expression in both Myc-CaP and 22Rv1 prostate cancer cells was low, and IGF-1 stimulation did not result in a clear increase in surface PD-L1 levels in 22Rv1 cells (Supplementary Figure S5B-C). While a modest shift in PD-L1 staining was observed in Myc-CaP cells following IGF-1 treatment, the overall MFI remained low compared to DU145 cells. As a result, we examined a colorectal adenocarcinoma cell line with high basal expression of both PD-L1 and IGF-1R. Testing IGF-1-induced expression in this cell line revealed a significant upregulation of PD-L1 surface expression (Supplementary Figure S5D), indicating that the IGF-1–PD-L1 axis is not restricted to prostate cancer but may extend to other malignancies. This IGF-1 induced effect was blocked by pre-treatment with actinomycin D (Fig. 3C, Supplementary Figure S5E-F) consistent with upregulation at the transcriptional level.

To investigate how IGF-1 contributes to PD-L1 regulation, we tested effects of inhibiting signaling pathways of IGF-1R and it's downstream effectors MEK-ERK and AKT in DU145 prostate cancer cells. Results suggest that blockade of IGF-1R, MEK-ERK or AKT suppressed IGF-induced PD-L1 upregulation at the transcriptional and cell surface level (Fig. 3D, Supplementary Figure S5G). Consistent with our findings, PD-L1 regulation by AKT and MEK was also reported in other human tumor cell lines[28,29].

IGF axis activity associates with deregulated immune genes and immune infiltrating cells in PCa tissues

To test the clinical relevance of these findings we interrogated public RNA-seq data from the Prostate Adenocarcinoma Firehose Legacy dataset in cbioportal (www.cbioportal.org/study/summary?id=prad_tcga)[30]. First, we tested associations of endogenous *IGF1* expression with *CD274* (PD-L1 mRNA), finding significantly higher *CD274* in tumours with the highest ($n = 124$) quartiles of IGF1 when compared with the lowest ($n = 125$; Fig. 4A). As a tissue indicator of IGF axis activation we also assessed IGF binding protein-5 (*IGFBP5*), a well-recognized transcriptional readout of IGF axis activity in many tissues and cell types[31]. Indeed, *IGFBP5* expression in this dataset was significantly higher in tumors with high endogenous *IGF1* mRNA, and reciprocally *IGF1* mRNA was higher in high *IGFBP5* tumors (Supplementary Figure S6A, B). Consistent with these associations of *IGF1* and *IGFBP5* mRNA, there was significantly higher *CD274* expression in Firehose LegacyPCatumors in the highest vs. lowest quartiles of *IGFBP5* (Fig. 4B). PCa Firehose Legacy tumors expressed low levels of *CTLA4*

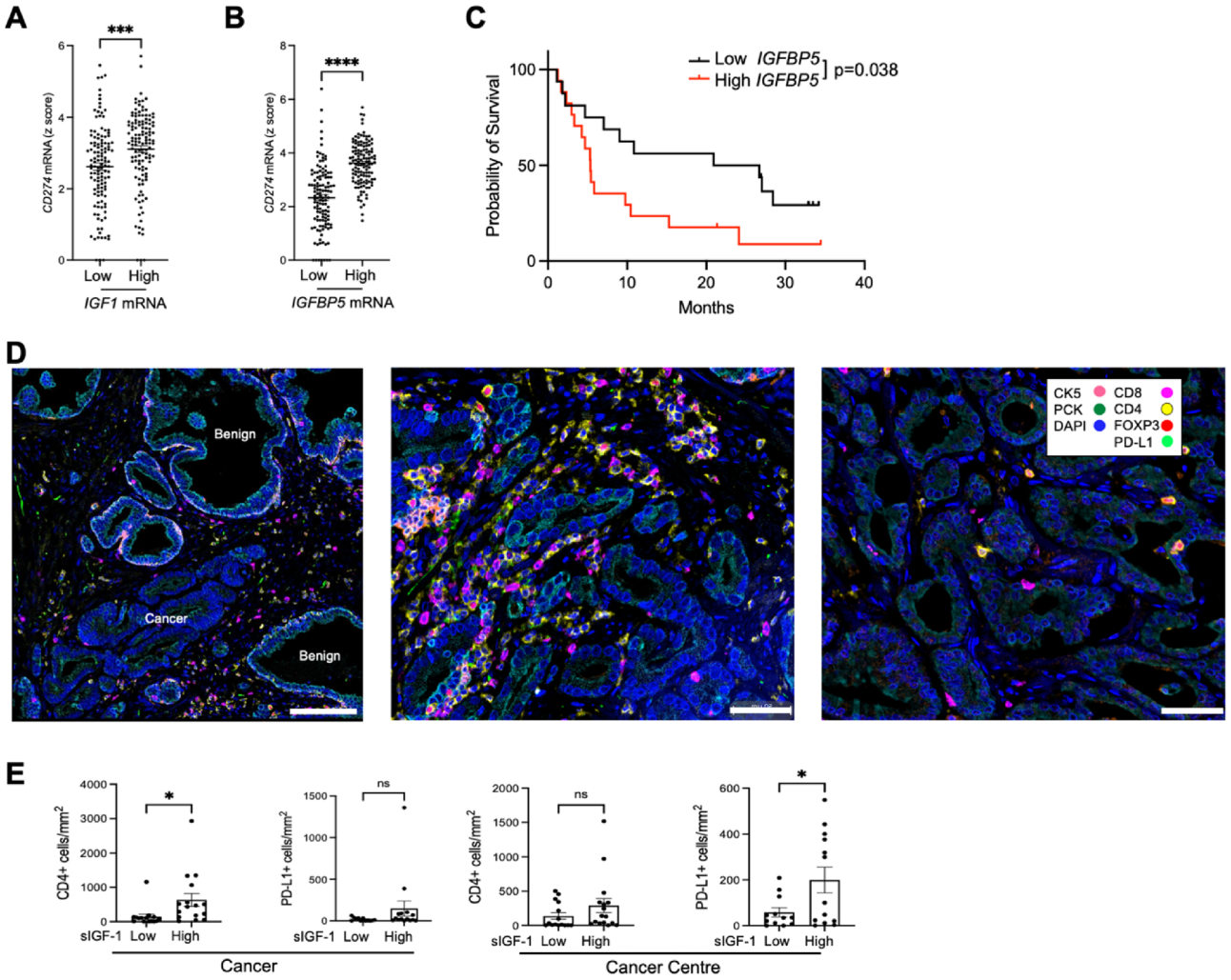

Fig. 4. IGF axis markers associate with altered expression of immune genes and immune infiltrating cells in clinical PCa tissue. **A-B.** Tumors from TCGA prostate adenocarcinoma Firehose Legacy dataset (n = 498) were divided based on highest and lowest quartiles of tumor endogenous *IGF1* or *IGFBP5* expression (n = low: 124, high = 125 in each case). Graphs show *CD274* expression (Z-score relative to all samples) in highest and lowest quartiles of *IGF1* (A) and I*GFBP5* (B). **C.** We accessed data from cbioportal on 110 ipilimumab -treated metastatic melanoma patients, of whom 40 had tumor transcriptional profiling[43]. These cases were divided by median *IGFBP5* (not quartiles due to small cohort size). Survival post-ICB censored at 36 months. Overall survival was significantly shorter (Log-rank (Mantel-Cox) test) in patients whose tumors expressed high *IGFBP5* (n = 17) vs. those with low *IGFBP5* melanomas (n = 16). **D.** Multiplex IF of radical prostatectomy tissue of ProMPT cases visualised using HALO. Representative images of: left, junction between benign glands (PCK + luminal cells surrounded by PCK+/CK5 + basal cells) and malignant epithelium (PCK+/CK5-, scale bar 100 µm); center: high immune infiltrating case; right: low immune infiltrating case (scale bar 50 µm). **E.** Quantification of CD4 + T-cells and PD-L1 positive cells in the total cancer area (left) and cancer center (right) in patients with high or low serum IGF-1. Graphs show mean ± SEM positively-stained cells (n = 31 for CD4 + staining, n = 25 for PD-L1, remaining cases lost due to technical issues with staining and visualization). (*p < 0.05; ***p < 0.001; ****p < 0.0001; ns, nonsignificant).

mRNA, and *CTLA4* transcript levels were significantly higher in tumors expressing high *IGFBP5* although not *IGF1* (Supplementary Figure S6C).

We searched for TCGA datasets that included transcriptional analysis and clinical survival data following ICB. We could not identify any datasets including anti-PD-1/PD-L1 therapy, but in a cohort of 110 patients with metastatic melanoma with survival data post anti-CTLA-4 ipilimumab, transcriptional profiles were available in 40. Patients whose tumors expressed high *IGFBP5* had significantly reduced overall survival (Fig. 4C). This is consistent with the reported contribution of the IGF axis to ICB resistance[19], although re-testing in larger cohorts will be required to confirm this finding.

As an additional approach to explore associations between the IGF axis and checkpoint expression, we returned to a cohort (n = 139) of men with localized PCa (n = 139) recruited between 2010 and 2014 to

Prostate Cancer: Mechanisms of Progression and Treatment (ProMPT study, MREC 01/4/061, PI F. Hamdy). We previously identified a transcriptional role for nuclear IGF-1R and association with advanced clinical stage[32]. Here, we assayed pre-prostatectomy serum IGF-1, finding that all values were within the normal range for adult men (Supplementary Figure S7A). We selected the 16 cases with the highest (21.74–31.49 nmol/L) and 16 with the lowest (7.19–11.98 nmol/L) IGF-1 and used FFPE prostatectomy sections for Multiplex immunofluorescence (mIF). The mIF panel comprised pancytokeratin (PCK) to stain prostate epithelium, cytokeratin 5 (CK5, expressed by basal cells of benign glands), and markers of helper T-cells (CD4+), cytotoxic T-cells (CD8+), regulatory T-cells (Tregs, FOXP3+) and PD-L1 (Fig. 4D). We first identified benign, tumor and central tumor regions of each tissue (Supplementary Figure S7B) and quantified immune and PD-L1 positive cells in each region. Many tumors had sparse immune infiltrates and there were no significant differences in total numbers of infiltrating CD8 + T-cells or FOXP3 + Tregs in the total tumor area or central tumor in high vs. low serum IGF-1 cases (Supplementary Figure S7C). However, central tumor of men with high serum IGF-1 contained more PD-L1 positive cells than tumors of men with low serum IGF-1 (Fig. 4E). This increase was observed in both epithelial cells (PCK + PD-L1+) and stromal cells (DAPI + PD-L1 + PCK- in stromal compartment) (Supplementary Figure S7C). These findings parallel the IGF-induced PD-L1 upregulation in cultured PCa cells (Fig. 3). In the total tumor area, there were also more T-cells positive for membrane CD4 in high serum IGF-1 cases compared with low IGF-1 cases (Fig. 4E).

Discussion

Our data indicate that IGF-1 regulates PCa expression of immune associated genes, components of the APM and the immune checkpoint PD-L1, with evidence of enriched and largely suppressed immune pathways. IGF-1 caused consistent downregulation of *TAP1*, *TAP2*, *ERAP1 and* β*2M*, suggesting perturbation of the APM. This effect was accompanied in Myc-CaP by TAP binding protein (*Tapbp*) downregulation. These data extend findings reported in HGG cells, where IGF-1 depletion rescued from downregulation of *TAP1*, *TAP2* and *LMP7*[33]. Furthermore, we identified significant IGF-induced reduction in presentation of cell surface Class I complexes by Myc-CaP cells. The lack of consistent changes in expression of Class I alleles in human or murine PCa cells suggests that the Class I upregulation and consequent CD8-dependent immune response reported in IGF-depleted or inhibited tumors[13,19] may be due not to reduced expression of MHC α-chains, but rather to disruption of peptide transport and processing, and downregulation of invariant Class I component β2M. In addition, *ERAP1* downregulation could influence trimming of Class I-bound precursor peptides, which in turn could affect the peptide repertoire and the conformational stability of Class I: peptide complexes[11]. As far as we are aware these changes have not been reported in PCa cells, although IGF-1 and insulin are reported to downregulate MHC Class I alleles in FRTL-5 rat thyroid cells and human hair follicle[34,35]. This suggests possible differences in Class I regulation between malignant and non-malignant cells and tissues.

The second concordant change related to *CD274*/PD-L1, reportedly expressed at low levels in primary PCa, with < 10% tumors containing IHC-detectable membrane PD-L1 in ≥1% of total cells in malignant epithelia and immune cells[36]. Consistent with this, there was evidence of generally low *CD274* mRNA in public PCa data although *CD274* expression was significantly higher in high *IGF1/IGFBP5* tumors (Fig. 4A-B) and at the protein level (mIF) in central tumor of men with high serum IGF-1 (Fig. 4E).

While IGFs are reported to have both pro- and anti- inflammatory actions, most reports favor an anti-inflammatory role. IGFs suppress cytokine secretion with anti-inflammatory associations in cardiac disease and diabetes[37,38]. Igf-1r activation is reported to suppress inflammation in the TME of NSCLC models[39] and induce degradation of retinoic acid-inducible gene-I (RIG1), a pattern-recognition receptor required for type 1 IFN production and the proper function of the innate immune response[40]. Several of our findings are consistent with an anti-inflammatory role in PCa. While single cell studies in IGF-manipulated tissue would be required to assess causality, these changes could suggest that IGF-induced transcriptional deregulation in PCa epithelium induces immunosuppression in components of the PCa TME.

Methods

Cells, reagents

Human PCa cell lines DU145 and 22Rv1 were from Cancer Research UK Laboratories (Clare Hall Hertfordshire UK) and Professor Sir Walter Bodmer (University of Oxford, UK) respectively. Human colorectal Adenocarcinoma cell lines H747 was purchased from ATCC. Cell lines were cryopreserved at early passage, regularly Mycoplasma tested and used within 20 passages. BMS-754,807, AZD5363 and trametinib were from Selleck Chemicals.

Reverse-transcription, quantitative PCR (qPCR)

RNA was extracted with the RNeasy kit (Qiagen) and reverse transcribed with SuperScript III First-Strand Synthesis SuperMix (Invitrogen). Gene expression was measured on the 7500 Fast Real-Time qPCR System (Thermo Fisher) using SYBR Green (New England Biolabs) and primers listed in Supplementary Table S1.

Flow cytometry

Cultured cells were dissociated with 2 mM Ethylenediamine tetra-acetic acid (EDTA, Sigma) in PBS at 37 °C, collected and washed in cold MACs buffer (0.5% bovine serum albumin, BSA, 2 mM EDTA in PBS). Cells were stained using antibodies listed in Supplementary Table S2 diluted in MACs buffer, then washed, fixed and stored in the dark at 4 °C. Surface expression was measured on the Attune NxT Flow Cytometer, data were analyzed using FlowJo 10.8.1 and expressed as % positivity and MFI.

Multiplex Immunofluorescence, HALO analysis

Multiplex immunofluorescence (mIF) was performed on 4 μm FFPE sections of radical prostatectomies from men recruited to the Prostate Cancer Mechanisms of Progression and Treatment (ProMPT) study, as described in[32] and mIF methods in[41], using Epitope Retrieval (ER) solutions, primary antibodies and their opal fluorophore pairings listed in Supplementary Table S2. Benign and cancer areas were annotated by Uro-Pathologist (CV), and areas of epithelium, stroma and artifact identified using the internal MiniNet AI classifier. Tumor margin, cancer and cancer center areas were annotated by HALO, and cells detected and signals quantified on the HALO HighPlex FL v3.1.0 module (Indica Labs).

RNA-sequencing (RNA-seq)

RNAs were quantified using RiboGreen (Invitrogen) on the FLUOstar OPTIMA plate reader (BMG Labtech) and size profile and integrity analyzed on the 2200 or 4200 TapeStation (Agilent, RNA ScreenTape). Input material was normalized to 20 ng, ribosomal RNA depleted using NEBNext rRNA Depletion Kit (NEB, Human/Mouse/Rat) and strand-specific library preparation used NEBNext Ultra II mRNA kit (NEB) following manufacturer's instructions. Libraries were amplified (17 cycles on Tetrad, Bio-Rad) using in-house unique dual indexing primers based on[42]. The size profile of individual libraries was analyzed on the 2200 or 4200 TapeStation and normalized using Qubit. Libraries were pooled, diluted to ~ 10 nM, denatured, and further diluted for paired-end sequencing (NovaSeq6000 platform, Illumina, NovaSeq 6000 S2/S4 reagent kit v1.5, 300 cycles).

Statistical and bioinformatic analysis

Using GraphPad Prism v9, we applied t-tests to calculate significance between two treatment groups, one-way ANOVA with Tukey's multiple comparison test for three or more treatment groups and Log-rank (Mantel-Cox) test for clinical survival data. Graphs show data from three independent experiments and p values < 0.05 were considered statistically significant. RNA-seq data were analyzed using software listed in Supplementary Table S3. The false discovery rate was controlled using the Benjamini-Hochberg (BH) method and results considered significant at adjusted p-value < 0.05. Gene set enrichment analysis (GSEA) used gene sets from the Molecular Signatures Database. For immune-focused analysis, we manually selected pathways from Gene Ontology (GO) Biological Processes, KEGG, BioCarta, WikiPathways, Reactome, and Hallmarks MsigDB collections, grouping them into three categories: cytokine, antigen processing/presentation and 'other immune-related'. Enrichment analysis used the clusterProfiler R package with BH multiple testing correction. Results were considered significant at adjusted p-value < 0.05, Venn diagrams and heatmaps were created with EnhancedVolcano, ggVennDiagram and ComplexHeatmap R packages, and GSEA plots with clusterProfiler (see Supplementary Table S3).

Data availability

All data underlying the findings presented in this manuscript can be found within the article and the Supplementary Information.

Received: 15 March 2025; Accepted: 26 September 2025
Published online: 03 November 2025

References

1. Chitnis, M. M., Yuen, J. S. P., Protheroe, A. S., Pollak, M. & Macaulay, V. M. The type 1 Insulin-Like growth factor receptor pathway. *Clin. Cancer Res.* **14**, 6364–6370. https://doi.org/10.1158/1078-0432.CCR-07-4879 (2008).
2. Hellawell, G. O. et al. Expression of the type 1 insulin-like growth factor receptor is up-regulated in primary prostate cancer and commonly persists in metastatic disease. *Cancer Res.* **62**, 2942–2950 (2002).
3. Turney, B. W., Turner, G. D. H., Brewster, S. F. & Macaulay, V. M. Serial analysis of resected prostate cancer suggests up-regulation of type 1 IGF receptor with disease progression. *BJU Int.* **107**, 1488–1499. https://doi.org/10.1111/j.1464-410X.2010.09556.x (2011).
4. Travis, R. C. et al. A Meta-analysis of individual participant data reveals an association between Circulating levels of IGF-I and prostate cancer risk. *Cancer Res.* **76**, 2288–2300. https://doi.org/10.1158/0008-5472.CAN-15-1551 (2016).
5. Watts, E. L. et al. Circulating insulin-like growth factor-I, total and free testosterone concentrations and prostate cancer risk in 200 000 men in UK biobank. *Int. J. Cancer.* **148**, 2274–2288. https://doi.org/10.1002/ijc.33416 (2021).
6. Kooijman, R. & Coppens, A. Insulin-like growth factor-I stimulates IL-10 production in human T cells. *J. Leukoc. Biol.* **76**, 862–867. https://doi.org/10.1189/jlb.0404248 (2004).
7. Bilbao, D., Luciani, L., Johannesson, B., Piszczek, A. & Rosenthal, N. Insulin-like growth factor-1 stimulates regulatory T cells and suppresses autoimmune disease. *EMBO Mol. Med.* **6**, 1423–1435. https://doi.org/10.15252/emmm.201303376 (2014).
8. Lopes, R. L., Borges, T. J., Zanin, R. F. & Bonorino, C. IL-10 is required for polarization of macrophages to M2-like phenotype by mycobacterial DnaK (heat shock protein 70). *Cytokine* **85**, 123–129. https://doi.org/10.1016/j.cyto.2016.06.018 (2016).
9. Vitkin, N., Nersesian, S., Siemens, D. R. & Koti, M. The tumor immune contexture of prostate cancer. *Front. Immunol.* **10**, 603. https://doi.org/10.3389/fimmu.2019.00603 (2019).
10. Trowsdale, J. Genomic structure and function in the MHC. *Trends Genet.* **9**, 117–122. https://doi.org/10.1016/0168-9525(93)90205-v (1993).
11. Mpakali, A., Maben, Z., Stern, L. J. & Stratikos, E. Molecular pathways for antigenic peptide generation by ER aminopeptidase 1. *Mol. Immunol.* **113**, 50–57. https://doi.org/10.1016/j.molimm.2018.03.026 (2019).
12. Taylor, B. C. & Balko, J. M. Mechanisms of MHC-I downregulation and role in immunotherapy response. *Front. Immunol.* **13**, 844866. https://doi.org/10.3389/fimmu.2022.844866 (2022).
13. Trojan, J. et al. Treatment and prevention of rat glioblastoma by Immunogenic C6 cells expressing antisense insulin-like growth factor I RNA. *Sci. (New York N Y).* **259**, 94–97 (1993).
14. Resnicoff, M. et al. Rat glioblastoma cells expressing an antisense RNA to the Insulin-like growth Factor-1 (IGF-1) receptor are nontumorigenic and induce regression of Wild-Type tumors. *Cancer Res.* **54**, 2218–2222 (1994).

15. Andrews, D. W. et al. Results of a pilot study involving the use of an antisense oligodeoxynucleotide directed against the insulin-like growth factor type I receptor in malignant Astrocytomas. *J. Clin. Oncol.* **19**, 2189–2200. https://doi.org/10.1200/JCO.2001.19.8.2189 (2001).
16. Andrews, D. W. et al. Phase Ib clinical trial of IGV-001 for patients with newly diagnosed glioblastoma. *Clin. Cancer Res.* **27**, 1912–1922. https://doi.org/10.1158/1078-0432.CCR-20-3805 (2021).
17. Nordstrand, A. et al. Inhibition of the insulin-like growth factor-1 receptor potentiates acute effects of castration in a rat model for prostate cancer growth in bone. *Clin. Exp. Metastasis.* **34**, 261–271. https://doi.org/10.1007/s10585-017-9848-8 (2017).
18. Xiong, D. et al. Immunogenomic Landscape Contributes to Hyperprogressive Disease after Anti-PD-1 Immunotherapy for Cancer. *iScience* 9, 258–277 (2018). https://doi.org/10.1016/j.isci.2018.10.021
19. Ajona, D. et al. Short-term starvation reduces IGF-1 levels to sensitize lung tumors to PD-1 immune checkpoint Blockade. *Nat. Cancer*. **1**, 75–85. https://doi.org/10.1038/s43018-019-0007-9 (2020).
20. Kang, B. et al. The novel IGF-1R inhibitor PB-020 acts synergistically with Anti-PD-1 and Mebendazole against colorectal cancer. *Cancers (Basel)*. 14. https://doi.org/10.3390/cancers14235747 (2022).
21. Hamilton, N. M. & LB-391-LB-391. Abstract LB-391: Combination of insulin-like growth factor-1 receptor/insulin receptor (IGF1R/IR) antagonist with anti-PD-L1 antibody blocks triple-negative breast cancer (TNBC) progression. *Cancer Research* 80, (2020). https://doi.org/10.1158/1538-7445.Am2020-lb-391
22. Watson, P. A. et al. Context-dependent hormone-refractory progression revealed through characterization of a novel murine prostate cancer cell line. *Cancer Res.* **65**, 11565–11571. https://doi.org/10.1158/0008-5472.CAN-05-3441 (2005).
23. Qiu, X. et al. MYC drives aggressive prostate cancer by disrupting transcriptional pause release at androgen receptor targets. *Nat. Commun.* **13**, 2559. https://doi.org/10.1038/s41467-022-30257-z (2022).
24. Sanda, M. G. et al. Molecular characterization of defective antigen processing in human prostate cancer. *J. Natl. Cancer Inst.* **87**, 280–285. https://doi.org/10.1093/jnci/87.4.280 (1995).
25. Groettrup, M., Standera, S., Stohwasser, R. & Kloetzel, P. M. The subunits MECL-1 and LMP2 are mutually required for incorporation into the 20S proteasome. *Proc. Natl. Acad. Sci. U S A*. **94**, 8970–8975. https://doi.org/10.1073/pnas.94.17.8970 (1997).
26. Sun, C., Zhang, N., Hu, Q. & Xia, G. Ferroptosis-Related prognostic gene LAMP2 is a potential biomarker differential expressed in castration resistant prostate cancer. *Dis. Markers*. **2023** (8295113). https://doi.org/10.1155/2023/8295113 (2023).
27. Marti, I. L. A. A. & Reith, W. Arginine-dependent immune responses. *Cell. Mol. Life Sci.* **78**, 5303–5324. https://doi.org/10.1007/s00018-021-03828-4 (2021).
28. Takahashi, A. et al. Tyrosine kinase inhibitors stimulate HLA class I expression by augmenting the IFNgamma/STAT1 signaling in hepatocellular carcinoma cells. *Front. Oncol.* **11**, 707473. https://doi.org/10.3389/fonc.2021.707473 (2021).
29. Zhang, S. et al. PD-L1 induction via the MEK-JNK-AP1 axis by a neddylation inhibitor promotes cancer-associated immunosuppression. *Cell. Death Dis.* **13**, 844. https://doi.org/10.1038/s41419-022-05292-9 (2022).
30. Gao, J. et al. Integrative analysis of complex cancer genomics and clinical profiles using the cBioPortal. *Sci. Signal.* **6** (pl1). https://doi.org/10.1126/scisignal.2004088 (2013).
31. Duan, C., Hawes, S. B., Prevette, T. & Clemmons, D. R. Insulin-like growth factor-I (IGF-I) regulates IGF-binding protein-5 synthesis through transcriptional activation of the gene in aortic smooth muscle cells. *J. Biol. Chem.* **271**, 4280–4288. https://doi.org/10.1074/jbc.271.8.4280 (1996).
32. Aleksic, T. et al. Nuclear IGF1R interacts with regulatory regions of chromatin to promote RNA polymerase II recruitment and gene expression associated with advanced tumor stage. *Cancer Res.* **78**, 3497–3509. https://doi.org/10.1158/0008-5472.CAN-17-3498 (2018).
33. Pan, Y., Trojan, J., Guo, Y. & Anthony, D. D. Rescue of MHC-1 antigen processing machinery by down-regulation in expression of IGF-1 in human glioblastoma cells. *PLoS One*. **8**, e58428. https://doi.org/10.1371/journal.pone.0058428 (2013).
34. Giuliani, C. et al. Transcriptional regulation of major histocompatibility complex class I gene by insulin and IGF-I in FRTL-5 thyroid cells. *J. Endocrinol.* **189**, 605–615. https://doi.org/10.1677/joe.1.06486 (2006).
35. Ito, T. et al. Collapse and restoration of MHC class-I-dependent immune privilege: exploiting the human hair follicle as a model. *Am. J. Pathol.* **164**, 623–634. https://doi.org/10.1016/S0002-9440(10)63151-3 (2004).
36. Haffner, M. C. et al. Comprehensive evaluation of programmed Death-Ligand 1 expression in primary and metastatic prostate cancer. *Am. J. Pathol.* **188**, 1478–1485. https://doi.org/10.1016/j.ajpath.2018.02.014 (2018).
37. Sukhanov, S. et al. IGF-1 reduces inflammatory responses, suppresses oxidative stress, and decreases atherosclerosis progression in ApoE-deficient mice. *Arterioscler. Thromb. Vasc Biol.* **27**, 2684–2690. https://doi.org/10.1161/ATVBAHA.107.156257 (2007).
38. Succurro, E. et al. Reciprocal association of plasma IGF-1 and interleukin-6 levels with cardiometabolic risk factors in nondiabetic subjects. *Diabetes Care*. **31**, 1886–1888. https://doi.org/10.2337/dc08-0553 (2008).
39. Alfaro-Arnedo, E. et al. IGF1R acts as a cancer-promoting factor in the tumor microenvironment facilitating lung metastasis implantation and progression. *Oncogene* **41**, 3625–3639. https://doi.org/10.1038/s41388-022-02376-w (2022).
40. Xie, Q. et al. Activation of insulin-like growth factor-1 receptor (IGF-1R) promotes growth of colorectal cancer through triggering the MEX3A-mediated degradation of RIG-I. *Acta Pharm. Sin B*. **13**, 2963–2975. https://doi.org/10.1016/j.apsb.2023.04.001 (2023).
41. Sivakumar, S. et al. Activated regulatory T-Cells, dysfunctional and senescent T-Cells hinder the immunity in pancreatic cancer. *Cancers (Basel)*. 13. https://doi.org/10.3390/cancers13081776 (2021).
42. Lamble, S. et al. Improved workflows for high throughput library Preparation using the transposome-based nextera system. *BMC Biotechnol.* **13**, 104. https://doi.org/10.1186/1472-6750-13-104 (2013).
43. Van Allen, E. M. et al. Genomic correlates of response to CTLA-4 Blockade in metastatic melanoma. *Science* **350**, 207–211. https://doi.org/10.1126/science.aad0095 (2015).

Acknowledgements

We dedicate this article to the memory of Prof. Valentine Macaulay, our group leader and co-lead author. Prof. Macaulay was not only a brilliant and dedicated scientist but also a compassionate mentor, an inspiring leader, and a cherished friend. Her unwavering commitment to science and her genuine care for those she worked with has left a profound mark on all of us. We feel fortunate to have had the privilege of calling her our colleague. This study was supported by Cancer Research UK Early Detection project grant (C476/A27060), Prostate Cancer UK awards (RIA-ST2-024 and MA-CT20-006), The Rosetrees Trust and John Black Foundation Charitable Trust (PhD-Plus award PhD2021-100025), Oxford University Human Immune Discovery Initiative (HIDI) fund, and UCARE-Oxford (GR280519). We gratefully acknowledge the contribution to this study made by the Oxford Centre for Histopathology Research and the Oxford Radcliffe Biobank, which are funded by the University of Oxford, the Oxford CRUK Cancer centre, the NIHR Oxford Biomedical Research Centre (BRC) (Molecular Diagnostics Theme/Multimodal Pathology Subtheme and the NIHR CRN Thames Valley network. The ProMPT study was supported by the UK NIHR, Cancer Research UK and the MRC, and the Cambridge and Oxford Biomedical Research Centres. The funding source had no role in the design, conduct of the study, collection, management, analysis and interpretation or preparation, review, or approval of the manuscript.

Author contributions

A.M.N. and V.M.M. designed experiments. A.M.N., J.K., C.R.L., J.V.M. and T.J., performed cell culture and *in vitro* experiments. D.D. and G.R. performed RNA Sequencing experiments. A.M.N., A.B., A.T. and A.J. performed bioinformatics analysis and visualization. F.C.M. and V.M.M. provided ethics and was responsible for clinical sample collection. T.J. conducted IGF-1 serum level analysis. C.V. annotated histopathology slides for analysis. L.C. performed multiplex imaging experiments. A.M.N. and A.E. performed analysis of the multiplex images. A.M.N. and V.M.M. wrote the manuscript. I.G.M., V.M.M., S.M.P., E.P. reviewed manuscript. A.M.N., G.R. and V.M.M. obtained funding. I.G.M. and V.M.M. provided supervision.

Declarations

Competing interests

The authors declare no competing interests.

Additional information

Supplementary Information The online version contains supplementary material available at https://doi.org/10.1038/s41598-025-22288-5.

Correspondence and requests for materials should be addressed to A.M.N.

Reprints and permissions information is available at www.nature.com/reprints.

Publisher's note Springer Nature remains neutral with regard to jurisdictional claims in published maps and institutional affiliations.